Chapter

Synthesis and Properties of Fluorinated Polyimides from Rigid and Twisted Bis(Trifluoromethyl) Benzidine for Flexible Electronics

Sun Dal Kim, Taejoon Byun, Jin Kim, Im Sik Chung and Sang Youl Kim

Abstract

Fluorinated polyimides were prepared from the twisted benzidine monomer containing two trifluoromethyl (CF_3) groups on one aromatic ring. The diamine monomer having a rigid and nonplanar structure was polymerized with typical dianhydride monomers including BPDA, BTDA, ODPA, 6-FDA, and PMDA, to obtain the corresponding polyimides. Most polyimides are soluble in organic solvents due to their twisted chain structure and can be solution cast into flexible and tough films. These films have a UV-vis absorption cut-off wavelength at 354–398 nm and a light transparency of 34–90% at a wavelength of 550 nm. They also have tensile strengths of 92–145 MPa and coefficients of thermal expansion (CTE) of 6.8–63.1 ppm/°C. The polymers exhibited high thermal stability with 5% weight loss at temperatures ranging from 535 to 605°C in nitrogen and from 523 to 594°C in air, and high glass temperature (T_g) values in the range of 345–366°C. Interestingly, some of the soluble polyimides showed thermo-responsive behaviors in organic solvents presumably due to the multiple hydrogen bondings with unsymmetrically positioned two CF_3 groups along the polymer chains.

Keywords: fluorinated polyimides, rigid and nonplanar structure, flexible and tough films, thermal stability, high glass temperature, coefficients of thermal expansion

1. Introduction

Aromatic polyimides (PIs) are well known as high-performance polymeric materials having excellent thermal, mechanical, and electrical properties. As a result of these properties, many PIs have been commercialized and used widely in microelectronic and aerospace engineering [1, 2]. Recently, aromatic PIs are considered as a strong candidate for flexible plastic substrates applicable to flexible electronics, including flexible solar cell arrays and flexible organic light-emitting diode (OLED) displays [3]. Despite the outstanding results associated with the use of aromatic PIs,

they also have a number of drawbacks, one of which is their poor processability caused by their limited degrees of solubility in organic solvents due to strong interchain interactions. Another shortcoming is the pale yellow or a deep brown color of PI films due to their highly conjugated aromatic structures and/or the formation of an intermolecular charge-transfer complex (CTC) between alternating electron-donor (diamine) and electron-acceptor (dianhydride) moieties, thus narrowing their applicability [4, 5].

To overcome these problems, much research effort has focused on the synthesis of soluble and transparent PIs in a fully imidized form without deterioration of their excellent properties [4, 6]. Several successful approaches to synthesize soluble and transparent PIs, including the insertion of flexible or unsymmetrical linkages or bulky substituents on the main chain and the use of noncoplanar or alicyclic monomers, have been introduced over the last few decades [4–8].

Among many approaches, the incorporation of trifluoromethyl (CF_3) groups onto polymer chains is considered as an effective means of realizing soluble and transparent PIs without deteriorating their excellent properties, not only because bulky CF_3 groups disturb the interactions and chain packing between the polymer chains, but also because the strength of the carbon-fluorine chemical bond is the one of the strongest single bonds [6, 9–30]. It is also possible to give the corresponding PIs have many attractive features, such as a low refractive index as well as low optical loss, dielectric constant, surface energy, and moisture absorption characteristics, due to the high electronegativity and low electric polarity of fluorine atoms [31–39].

Recently, we reported new soluble PIs which were prepared from 4-(4′-aminophenoxy)-3,5-bis(trifluoromethyl)aniline to introduce two CF_3 groups unsymmetrically onto the repeating units of the chain [40, 41]. Unsymmetrical incorporation of the substituents into the main chain of PIs can improve the solubility and optical transparency because increasing the irregularity of the microstructure of PIs disrupts the interchain interactions [42–47]. The PIs synthesized in earlier work showed good solubility while retaining their useful thermal and optical properties due to the unsymmetrical presence of CF_3 groups as substituents. Furthermore, the good solubility of the PIs led them to show lower critical solution temperature (LCST) behavior in organic solvents. This unprecedented phenomenon of the PIs may stem from a change of the interaction strength in the vicinity of CF_3 between the polymer chains and the acetyl-containing solvents [41].

Subsequently, we designed another monomer, 2,6-bis(trifluoromethyl) benzidine, which has two CF_3 groups at the 2,6-positions of the benzidine unit [48]. Although this monomer has more rigid structure compared to 4-(4′-aminophenoxy)-3,5-bis(trifluoromethyl)aniline, a series of poly(amide-imide)s synthesized from the monomer exhibited good solubility as well as good thermal and optical properties. Meanwhile, in terms of the structure, the new benzidine monomer has an isomeric relationship with 2,2′-bis(trifluoromethyl)benzidine, well known as a rigid/linear benzidine unit containing the CF_3 group and frequently employed in the synthesis of PIs having a high thermal resistance, a high T_g value, a low degree of thermal expansion, a low refractive index, and low water absorption capabilities [16–30]. Therefore, we envisioned that the PIs obtained from the new benzidine monomer would exhibit high thermal and mechanical properties while maintaining good solubility in organic solvents, as they have twisted structures while retaining the rigidity of the chains. The chemistry and the physical properties of the PIs prepared from the twisted benzidine monomer containing two trifluoromethyl (CF_3) groups on one aromatic ring are described herein.

2. Experiments

2.1 Materials

2-Bromo-5-nitro-1,3-bis(trifluoromethyl)benzene (**1**) and 2,6-bis (trifluoromethyl)benzidine (**3**) were synthesized as reported in our previous papers [31, 48]. The aromatic tetracarboxylic dianhydrides of pyromellitic dianhydride (PMDA), 3,3′,4,4′-biphenyltetracarboxylic dianhydride (BPDA), 3,3′,4,4′-benzophenone-tetracarboxylic dianhydride (BTDA), 4,4′-oxydiphthalic anhydride (ODPA), and 4,4′-hexafluoroisopropylidenediphthalic anhydride (6-FDA) were purified by vacuum sublimation. *m*-Cresol was stirred in the presence of P_2O_5 overnight and then distilled under reduced pressure. All other commercially available reagent-grade chemicals were used without further purification.

2.2 Measurements

The Fourier-transform infrared (FTIR) spectra of the compounds were obtained with a Bruker EQUINOX-55 spectrophotometer using a KBr pellet or film. The nuclear magnetic resonance (NMR) spectra of the synthesized compounds were recorded on a Bruker Fourier Transform Avance 400 spectrometer. The chemical shift of the NMR was reported in parts per million (ppm) using tetramethylsilane as an internal reference. Splitting patterns were designated as s (singlet), d (doublet), dd (doublet of doublets), dt (doublet of triplets), t (triplet), q (quartet), or m (multiplet). Elemental analyses (EA) of the synthesized compounds were carried out with a FLASH 2000 series device. The single-crystal diffraction data of the diimide model compound were collected on a Bruker SMART 1000 with graphite-monochromated Mo Kα radiation (λ = 0.71073 Å) at 120 K. The inherent viscosities of the polymers were measured using an Ubbelohde viscometer. Gel permeation chromatography (GPC) diagrams were obtained with a Viscotek TDA302 instrument equipped with a packing column (PLgel 10 μm MIXED-B) using tetrahydrofuran (THF) as an eluent at 35°C. The number and weight-average molecular weight of the polymers were calculated relative to linear polystyrene standards. Wide-angle X-ray diffraction (WAXD) measurements were performed at room temperature (ca. 25°C) on a Rigaku D/MAX-2500 X-ray diffractometer with a Cu Kα radiation under graphite monochromatic operation at 40 kV and 300 mA. The scanning rate was 1°/min over a range of 2θ = 2–45°. The mechanical properties of the films were measured with an Instron 5567 at a crosshead speed of 2 mm/min on strips approximately 40–50 μm thick and 11 mm wide with a 15 mm gauge length. The average of two individual determinations was used. Thermogravimetric analysis (TGA) and differential scanning calorimetry (DSC) were conducted on a TA Instruments TGA Q500 and a DSC Q100 instrument, respectively. The TGA measurements were conducted at a heating rate of 10°C/min in N_2 and air. The melting points (m.p.) of the synthesized compounds and the T_g values of the polymers were obtained with DSC instrument at a heating rate of 10°C/min in N_2. T_g values were taken from the second heating scan after cooling to 0°C from 400°C. The in-plane linear coefficients of thermal expansion (CTEs) of polymer films were measured by thermomechanical analysis (TMA) using a TA TMA-2940 thermomechanical analyzer. Specimens were 5 mm in width, 10 mm in length, and typically 70 μm thick. The measurements were carried out three times in a heating range up to 300°C at a heating rate of 5°C/min. After the first measurement (first run), the sample was cooled gradually to room temperature in a nitrogen atmosphere, after which the second measurement (second run) was taken. The same operation was carried out

between the second run and the third run. The CTE values were determined as the mean at 50–250°C in the second and third heating runs. UV-visible spectra of the polymer films were recorded on an Optizen POP spectrophotometer in the transmittance mode. The refractive indices n_{TE} and n_{TM} for the transverse electric (TE) and transverse magnetic (TM) modes of the polymer films were measured with a Sairon SPA-4000 prism coupler equipped with a gadolinium gallium garnet (GGG) prism at a wavelength of 633 nm at room temperature. The birefringence values (Δn) were calculated as the difference between n_{TE} and n_{TM}. In order to confirm the thermal response behavior of the polymers in organic solvents, another UV-vis spectrophotometer (Shimadzu UV-3600) was used. The transmittance change was measured at a wavelength of 600 nm, and the heating and cooling rates were 0.5°C/min. The clouding point (T_{cp}) was determined as the temperature at which 90% transmittance was observed during the heating process. When T_{cp} was observed at a temperature above the boiling temperature of the solvent used, T_{cp} was measured by the naked eye, while the solutions were placed in screw-cap vials and gradually heated at 5°C intervals in a heating bath equipped with a mercury thermometer.

2.3 Polymerization

PI-1. Diamine monomer **3** (0.4012 g, 1.253 mmol) and BPDA (0.3689 g, 1.254 mmol) were initially dissolved in 4.8 mL of *m*-cresol to a concentration of 16 wt% in a 25 mL three-necked round-bottom flask equipped with a nitrogen inlet, a Dean-Stark trap, and a mechanical stirrer. After the mixture was stirred at room temperature for 30 min, isoquinoline (ca. 5 drops) was added, and further stirring was conducted at room temperature for 4 h. After the solution was diluted with 4.8 mL of *m*-cresol to a concentration of 8 wt%, the temperature was raised to 190°C slowly and the reaction mixture was stirred for 12 h at this temperature. During this time, the water released during the imidization process was removed by distillation as chlorobenzene/water azeotrope, and small amount of *m*-cresol (total additional volume = 4.8 mL) was added periodically to maintain proper viscosity of the reaction mixture. After cooling to room temperature, the solution was diluted with *m*-cresol and then slowly poured into an excess of vigorously stirred ethanol. The resulting polymer was collected by filtration, washed with ethanol, and then dried in vacuo at 180°C for 12 h (0.7444 g, 100% yield). FTIR (thin film, cm^{-1}): 1779 (asym C═O str); 1726 (sym C═O str); 1476 (aromatic C═C); 1373 (C—N str); 1123–1190 (C—F in CF_3); 738 (imide ring deformation). ^{1}H NMR (DMSO-d_6, 400 MHz, 100°C, ppm): 8.54–8.34 (m, 6H), 8.25–8.04 (m, 2H), 7.66 (d, J = 8.1 Hz, 2H), 7.56 (d, J = 8.5 Hz, 2H). ^{1}H NMR (THF-d_8, 400 MHz, 55°C, ppm): 8.49 (d, J = 18.6 Hz, 2H), 8.37 (s, 4H), 8.24–8.08 (m, 2H), 7.73 (d, J = 7.9 Hz, 2H), 7.51 (d, J = 8.6 Hz, 2H). Anal. calcd for $C_{30}H_{12}F_6N_2O_4$: C, 62.29; H, 2.09; N, 4.84. Found: C, 61.51; H, 2.06; N, 4.78.

PI-2. The same procedure used for **PI-1** was repeated with 0.4017 g (1.254 mmol) of **3**, 0.4043 g of (1.255 mmol) of BTDA, and 5 mL of *m*-cresol. Before heating the reaction mixture to 190°C, the solution was diluted with 5 mL of *m*-cresol and there was no injection of the additional solvent (0.7538 g, 99.1% yield). FTIR (thin film, cm^{-1}): 1783 (asym C═O str); 1732 (sym C═O str); 1679 (diaryl ketone of BTDA); 1476 (aromatic C═C); 1376 (C—N str); 1137–1191 (C—F in CF_3); 723 (imide ring deformation). ^{1}H NMR (DMSO-d_6, 400 MHz, 25°C, ppm): 8.40 (s, 2H), 8.35–8.14 (m, 6H), 7.60 (s, 4H). Anal. calcd for $C_{31}H_{12}F_6N_2O_5$: C, 61.40; H, 1.99; N, 4.62. Found: C, 61.20; H, 2.08; N, 4.44.

PI-3. The same procedure used for **PI-1** was repeated with 0.4030 g of (1.258 mmol) of **3**, 0.3907 g (1.259 mmol) of ODPA, and 4.9 mL of *m*-cresol. Before heating the reaction mixture to 190°C, the solution was diluted with 4.9 mL of

m-cresol and there was no injection of the additional solvent (0.7548 g, 100% yield). FTIR (thin film, cm^{-1}): 1782 (asym C═O str); 1729 (sym C═O str); 1475 (aromatic C═C); 1375 (C—N str); 1276, 1239 (—O—); 1140–1190 (C—F in CF_3); 745 (imide ring deformation). ^1H NMR (DMSO-d_6, 400 MHz, 25°C, ppm): 8.36 (s, 2H), 8.14 (dt, J = 17.8, 6.7 Hz, 2H), 7.77–7.62 (m, 4H), 7.56 (s, 4H). Anal. calcd for $C_{30}H_{12}F_6N_2O_5$: C, 60.62; H, 2.03; N, 4.71. Found: C, 60.71; H, 2.01; N, 4.66.

PI-4. The same procedure used for **PI-1** was repeated with 0.4003 g (1.250 mmol) of **3**, 0.5560 g (1.252 mmol) of 6-FDA, and 6 mL of *m*-cresol. Before heating the reaction mixture to 190°C, the solution was diluted with 6 mL of *m*-cresol without injection of any additional solvent (0.8961 g, 98.4% yield). FTIR (thin film, cm^{-1}): 1789 (asym C═O str); 1733 (sym C═O str); 1476 (aromatic C═C); 1375 (C—N str); 1145–1193 (C—F in CF_3); 722 (imide ring deformation). ^1H NMR (DMSO-d_6, 400 MHz, 25°C, ppm): 8.34 (s, 2H), 8.28 (t, J = 7.8 Hz, 1H), 8.23 (t, J = 8.0 Hz, 1H), 8.04 (t, J = 6.6 Hz, 1H), 7.98 (t, J = 6.2 Hz, 1H), 7.80 (dd, J = 18.6, 15.8 Hz, 2H), 7.56 (s, 4H). Anal. calcd for $C_{33}H_{12}F_{12}N_2O_4$: C, 54.41; H, 1.66; N, 3.85. Found: C, 55.43; H, 1.56; N, 3.77.

PI-5. The same procedure used for **PI-1** was repeated with 0.4062 g (1.268 mmol) of **3**, 0.2768 g (1.269 mmol) of PMDA, and 4.2 mL of *m*-cresol. After the solution was diluted with 4.2 mL of *m*-cresol to a concentration of 8 wt%, the temperature was raised to 190°C slowly. The solution became turbid and heterogeneous as soon as the temperature reached 190°C. The heterogeneous reaction mixture was further stirred for 12 h at this temperature. After cooling to room temperature, the solution was poured into an excess of vigorously stirred ethanol. The solid polymer powder was collected by filtration, washed with ethanol, and then dried in vacuo at 180°C for 12 h (0.6392 g, 100% yield). FTIR (KBr, cm^{-1}): 1783 (asym C═O str); 1728 (sym C═O str); 1477 (aromatic C═C); 1367 (C—N str); 1125–1192 (C—F in CF_3); 724 (imide ring deformation). Anal. calcd for $C_{24}H_8F_6N_2O_4$: C, 57.38; H, 1.61; N, 5.58. Found: C, 56.81; H, 1.70; N, 5.46.

2.4 Preparation of polyimide films

An *N*,*N*-dimethylacetamide (DMAc) solution of the polymers (7.5 wt%) was prepared at room temperature. The DMAc solution was filtered and cast onto a glass plate. The solvent was evaporated in a vacuum oven at room temperature for 5 h and then heated to 180°C for 10 h to remove the residual solvent. To measure the refractive indices of the polyimides, the DMAc solution of the polymers (2.5 wt%) was filtered and cast onto a silicon substrate and then dried in the same manner described above.

3. Results and discussion

3.1 Monomer syntheses

The diamine monomer, 2,6-bis(trifluoromethyl)benzidine (**3**), was prepared in two steps, as reported previously (**Figure 1**) [48]. In the first step, 2-bromo-5-nitro-1,3-bis(trifluoromethyl)benzene (**1**) was reacted with 4-aminophenylboronic acid through a Suzuki coupling reaction in the presence of Pd as a catalyst to produce **2**. The mono-nitro compound was quantitatively converted to the corresponding diamine monomer **3** by hydrogenation with hydrogen in the presence of Pd/C catalyst.

The chemical structures of **2** and **3** were confirmed by ^1H and ^{13}C NMR, FTIR, and an elemental analysis. **Figure 2** shows the NMR spectra of **2** and **3**. Through a reduction reaction, the chemical shifts of proton H_1 and carbon C_1 moved upfield because they were more shielded by the change of the substituents from the NO_2

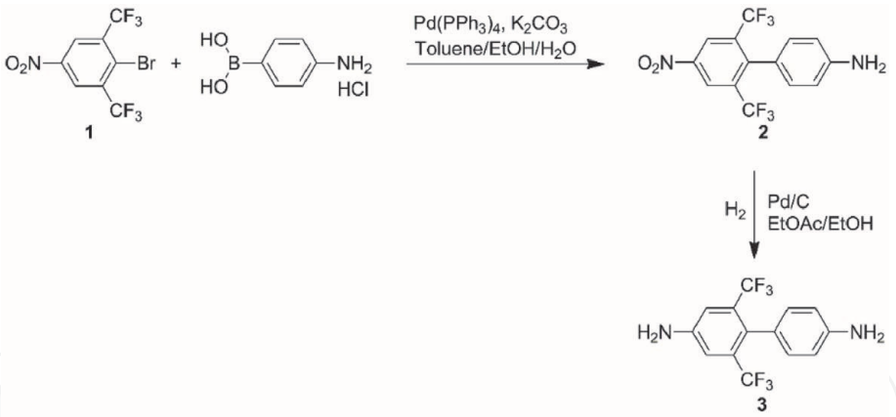

Figure 1.
Synthesis of the unsymmetrical diamine monomer.

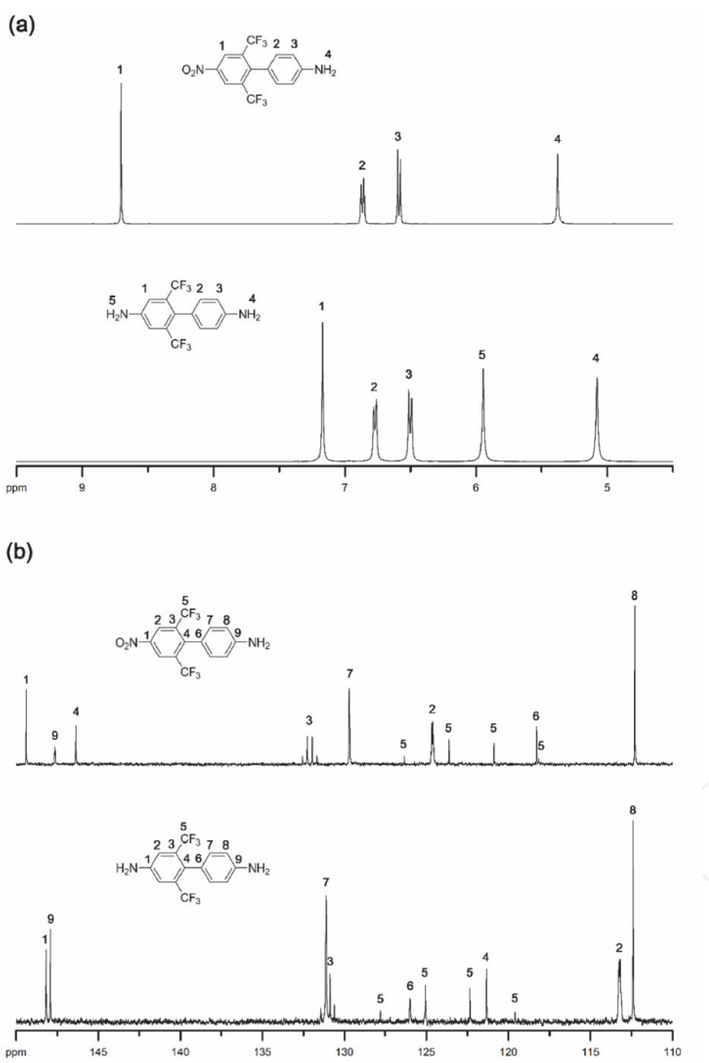

Figure 2.
(a) ^{1}H and (b) ^{13}C NMR spectra of **2** *and* **3** *(DMSO-*d_6*, 25°C) [48].*

group to the NH_2 group. Meanwhile, there were obvious differences in the chemical shifts between the two amine groups in monomer **3**. The chemical shifts of proton H_5 and carbon C_1 in **3** appear further downfield compared to those of H_4 and C_9 due to the deshielding effect of the electron withdrawing CF_3 groups, indicating that the amine group located far away from CF_3 groups in monomer **3** has a higher electron density and greater nucleophilic reactivity than in the opposite case. The FTIR

spectra of **2** and **3** are shown in **Figure 3**. The compound **2** gave characteristic bands at 3499, 3401 cm^{-1} (N—H stretching), at 1620 cm^{-1} (N—H bending), and at 1333–1533 cm^{-1} (NO_2 asymmetric and symmetric stretching). After the reduction, the characteristic absorptions of the nitro group disappeared, and the amino group exhibited a pair of N—H stretching bands in the region of 3221–3486 cm^{-1} and an N—H bending band at 1640 cm^{-1}. All spectroscopic data obtained were in good agreement with the predicted structures.

3.2 Model reaction

A model reaction was conducted to investigate the suitability of a nucleophilic addition and cyclodehydration of the diamine monomer in the polymerization reaction condition as well as to obtain a model compound as a reference material for a structural analysis. The diamine monomer was reacted with two-equivalent of phthalic anhydride in *m*-cresol in the presence of a catalytic amount of isoquinoline

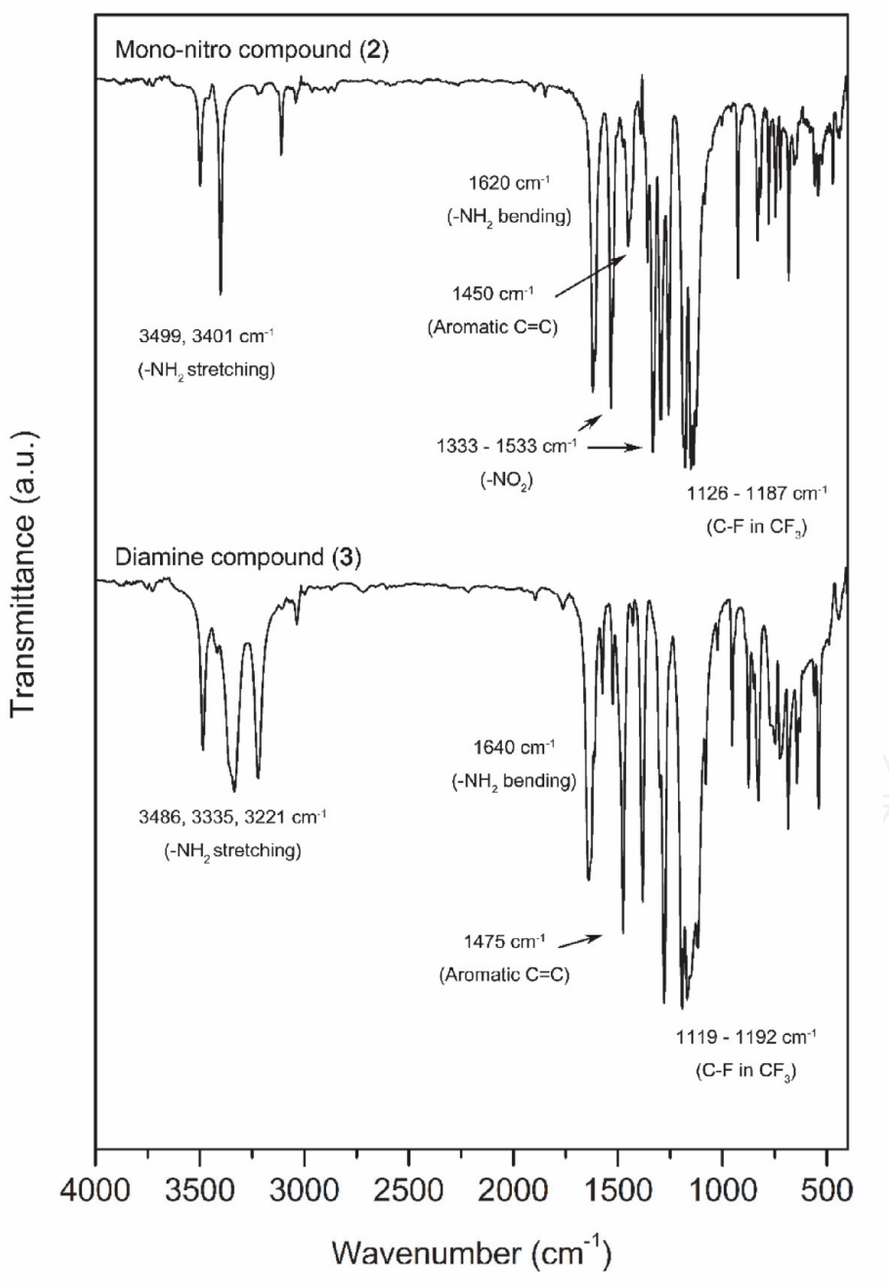

Figure 3.
FTIR spectra of mono-nitro (2) and diamine (3) compounds [48].

(**Figure 4**), and all reaction steps were examined by thin layer chromatography. Despite the difference in the electron density between the two amines resulting from the unsymmetrical structure, the two amines had sufficient nucleophilicity to react with the phthalic anhydride. As a result, the corresponding diamic acid form was generated quantitatively within 0.5 h at room temperature, and cyclodehydration was completed within 0.5 h at 190°C. Finally, diimide model compound (**4**) was obtained quantitatively. The structure of **4** was confirmed by FTIR, ^{1}H NMR and ^{13}C NMR spectroscopy (**Figure 5**). The FTIR spectrum of the model compound shows absorption bands at 1789, 1380, and 722 cm^{-1} corresponding to the C═O imide stretching, C—N imide stretching, and imide ring deformation, respectively, without the characteristic absorptions of the amino groups. The ^{1}H and ^{13}C NMR spectra also supported the formation of the diimide model compound. Owing to the unsymmetrical presence of CF_3 groups on the product, proton and carbon peaks on both phthalimide units appeared with different chemical shifts in the NMR spectra, in which the peaks of phthalimide connected to a trifluoromethylated phenyl ring appeared further downfield due to the electron-withdrawing characteristic of the CF_3 groups. All spectroscopic data obtained were in good agreement with the predicted structure.

The structure features of **4** were further detailed by single-crystal X-ray diffraction, and its X-ray quality crystals were obtained by the slow evaporation of saturated tetrahydrofuran/water solution at room temperature [48]. As shown in **Figure 6**, the solid-state structure of **4** also ensures the coupling reaction of **3** to the phthalic anhydrides. It is noteworthy that the plane of a phenyl moiety is almost orthogonally located relative to the adjacent *m*-$(CF_3)_2$Ph plane such that the biphenyl of **4** had a rigid but twisted structure with a dihedral angle (θ) of 76°. Compared with 2,2′-bis(trifluoromethyl)benzidine (θ = 59°) [27], the benzidine unit of **4** is more distorted. Therefore, it was expected that the obtained polyimides would exhibit good solubility and transparency with high mechanical and thermal properties, as they have a rigid but twisted structure with bulky CF_3 groups, thereby reducing the interchain interactions.

3.3 Polymer syntheses

Based on the results of the model reactions, several polyimides (PIs) were prepared from **3** and commercially available aromatic dianhydrides via a one-pot solution imidization method, as shown in **Figure 7**. The polymerizations of diamine

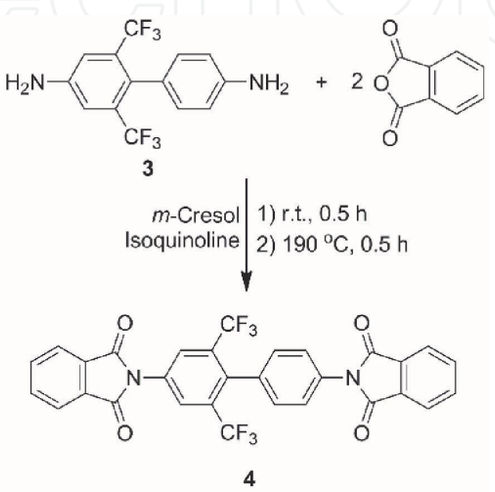

Figure 4.
Model reaction of 3 with phthalic anhydride.

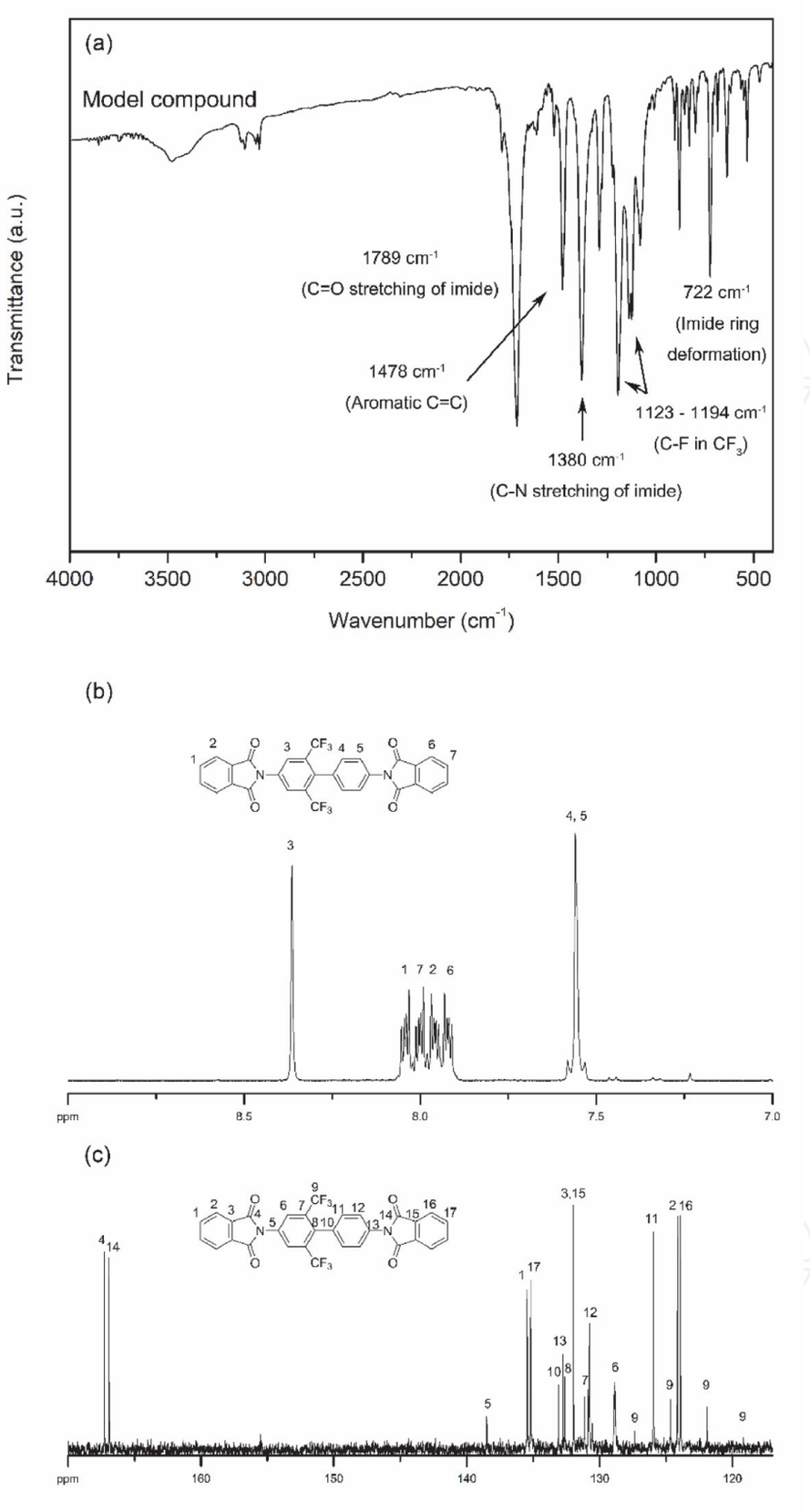

Figure 5.
*(a) FTIR, (b) ^{1}H, and (c) ^{13}C NMR spectra of model compound (**4**) (NMR: DMSO-d_6, 25°C) [48].*

monomer **3** with stoichiometric amounts of five different aromatic dianhydride monomers, BPDA (**PI-1**), BTDA (**PI-2**), ODPA (**PI-3**), 6-FDA (**PI-4**), and PMDA (**PI-5**), were carried out in *m*-cresol with catalytic amounts of isoquinoline at a solid content of about 16 wt%. The ring-opening polyaddition at room temperature for

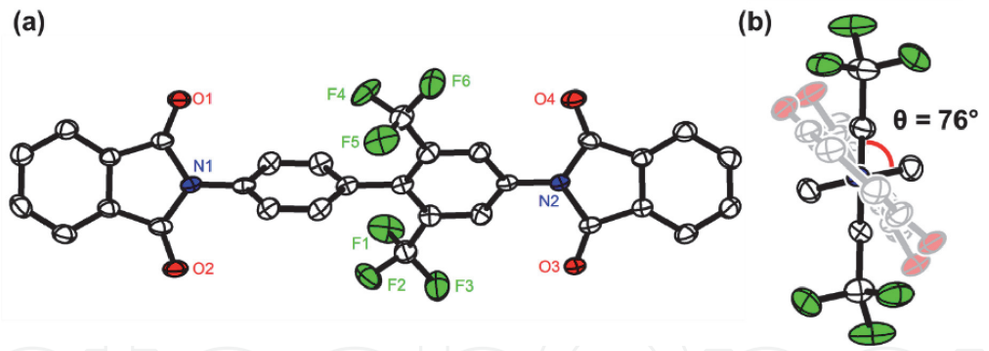

Figure 6.
(a) Top view and (b) side view of displacement ellipsoid (50%) representations of ***4****. All hydrogen atoms are omitted for clarity.*

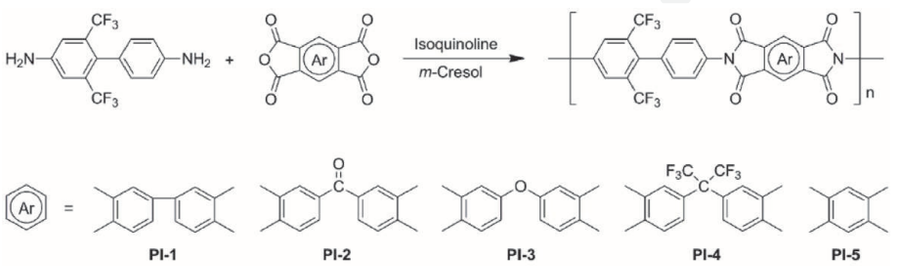

Figure 7.
Polymerization of ***3*** *with aromatic dianhydrides.*

4 h yielded poly(amic acid) solutions. After dilution of the solution to 8 wt%, subsequent cyclodehydration by heating at 190°C with the azeotropic distillation of chlorobenzene for 12 h gave fully imidized and homogeneous PI solutions except for that of PMDA (**PI-5**). When PMDA was used as the dianhydride, the solution became turbid with phase separation as soon as the temperature reached 190°C. This was likely due to the most rigid chain characteristic of **PI-5**. At the end of the reaction, pure solid polymers were obtained by precipitation of the corresponding polymer solutions into ethanol.

Table 1 shows the inherent viscosities and GPC data of the PIs. The inherent viscosities of the organosoluble PIs were in the range of 0.69–2.30 dL/g, as measured in DMAc at 30°C. Additionally, the PIs soluble in THF exhibited weight-average molecular weights (M_ws) in the range of 7.32–8.81 × 10^4 relative to the polystyrene standard. The molecular weights of the PIs were high enough to obtain flexible and tough polymer films by casting from their DMAc solutions.

The formation and the structures of the polymers were verified by elemental analyses, FTIR, and ^{1}H NMR spectroscopy. The elemental analysis values of the PIs (listed in Experiments) were in good agreement with the calculated values of the proposed structures. The typical FTIR spectrum of **PI-1** is shown in **Figure 8**. All PIs exhibited characteristic imide group absorptions around 1780 and 1730 (typical of imide carbonyl asymmetrical and symmetrical stretching), 1370 (C—N stretching), and 730 cm^{-1} (imide ring deformation), together with a number of strong absorption bands in the regions of 1120–1200 cm^{-1} due to C—F stretching. The absence of amide and carboxyl bands indicates the virtually complete conversion of the poly (amic acid) precursors into PIs. The ^{1}H NMR spectra of the PIs are illustrated in **Figure 9**. All proton peaks were also assigned to the predicted structures without amide and acid protons, demonstrating the successful preparation of the PIs. Additionally, the proton peaks of the dianhydride units in the polymer chains were divided into different chemical shifts due to the unsymmetrical structure of the diamine unit in the PI main chains. The chemical shifts of protons closer to the CF_3

Polymer code	η_{inh} (dL/g)[a]	M_w (kDa)[b]	M_n (kDa)[b]	M_w/M_n[b]
PI-1	2.30	—[c]	—[c]	—[c]
PI-2	0.78	73.2	28.2	2.60
PI-3	0.88	83.7	33.6	2.49
PI-4	0.69	88.1	32.9	2.68
PI-5	—[c]	—[c]	—[c]	—[c]

[a]*Measured in DMAc at a concentration of 0.5 g/dL at 30°C.*
[b]*Determined by GPC in THF at 35°C (relative to polystyrene standard).*
[c]*Insoluble.*

Table 1.
Inherent viscosities and elemental analyses results of the PIs.

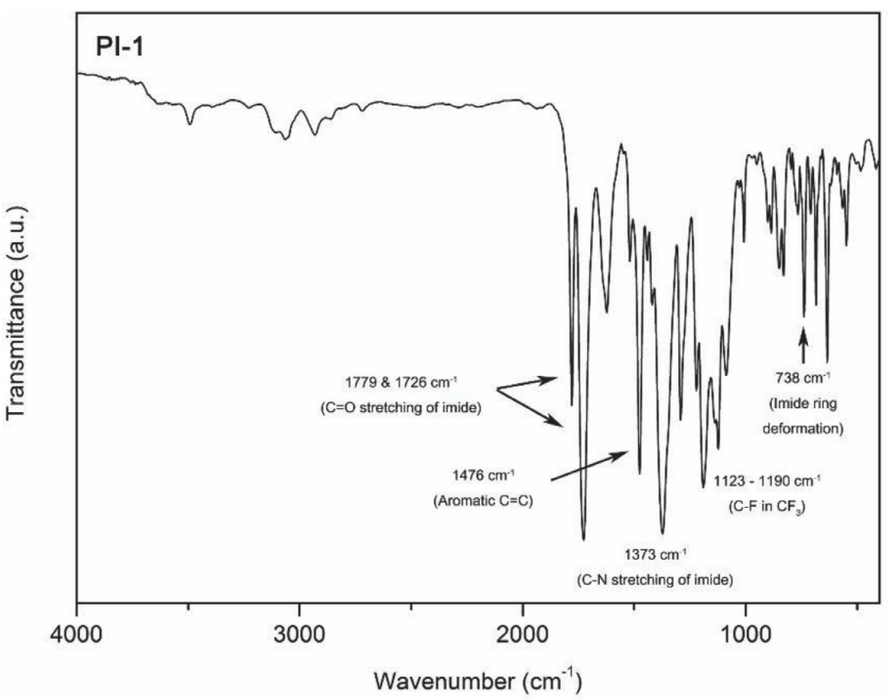

Figure 8.
*FTIR spectrum of **PI-1** (film).*

groups appeared further downfield in the NMR spectrum due to the deshielding effect of the electron-withdrawing CF_3 groups. This result was consistent with the model reaction result.

3.4 Polymer properties

The solubility of the synthesized PIs is summarized in **Table 2**. The synthesized polymers retained good solubility in organic solvents, although their rigidity increased compared to those synthesized from 4-(4′-aminophenoxy)-3,5-bis (trifluoromethyl)aniline [40]. All PIs except for **PI-5** exhibited good solubility in *N*-methyl-2-pyrrolidone (NMP), *N*,*N*-dimethylacetamide (DMAc), *m*-cresol, and anisole at room temperature. In addition, **PI-2**, **PI-3**, and **PI-4** showed good solubility in *N*,*N*-dimethylformamide, dimethyl sulfoxide, tetrahydrofuran, and ethyl acetate at room temperature. The good solubility of the PIs is attributed not only to the bulkiness of the two CF_3 groups on the polymer chains but also to the unsymmetrical structure resulting from the diamine monomer. Given the increased chain flexibility, **PI-3** and **PI-4** were also soluble in chloroform and **PI-4** was soluble even

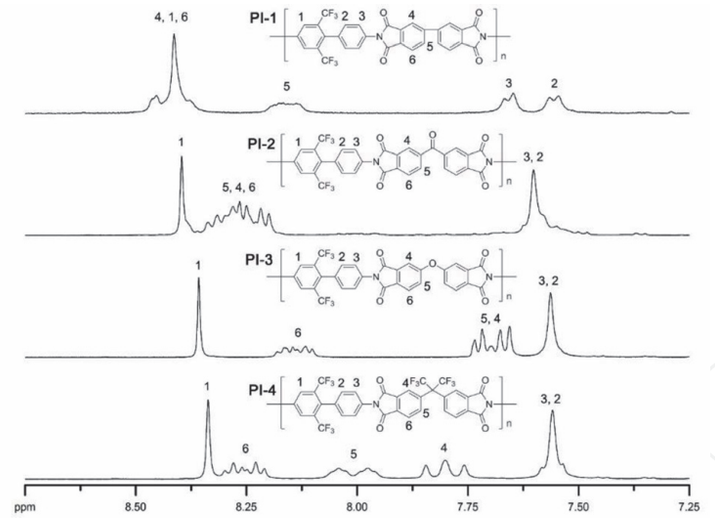

Figure 9.
*^{1}H NMR spectrum of **PI-1** (DMSO-d_6, 100°C); ^{1}H NMR spectra of **PI-2**, **PI-3**, and **PI-4** (DMSO-d_6, 25°C).*

Solvents	PI-1	PI-2	PI-3	PI-4	PI-5
NMP	++	++	++	++	+−
DMAc	++	++	++	++	+−
m-Cresol	++	++	++	++	−
Anisole	++	++	++	++	−
DMF	+	++	++	++	−
DMSO	+	++	++	++	−
THF	+	++	++	++	−
Ethyl acetate	−	++	++	++	−
Acetone	−	+−	+−	++	−
Chloroform	−	−	++	++	−
ODCB	+	+	+	+	−
Acetonitrile	−	−	−	−	−
Toluene	−	−	−	−	−
Diethyl ether	−	−	−	−	−
n-Hexane	−	−	−	−	−
Methanol	−	−	−	−	−

Solubility: ++, soluble at room temperature; +, soluble on heating; +−, partially soluble; −, insoluble. Abbreviations: NMP, N-methyl-2-pyrrolidone; DMAc, N,N-dimethylacetamide; DMF, N,N-dimethylformamide; DMSO, dimethyl sulfoxide; THF, tetrahydrofuran; ODCB, 1,2-dichlorobenzene.

Table 2.
Solubility of the PIs.

in acetone at room temperature. Upon a comparison of the solubility behavior with PIs prepared from symmetrical benzidine, 2,2′-bis(trifluoromethyl)benzidine [17–21], the PIs described here showed enhanced solubility. The improved solubility can be attributed to the unsymmetrical and more twisted chain structure, which inhibits close packing and reduces intermolecular interactions. Meanwhile, **PI-5** showed poor solubility in the organic solvents tested, although it was partially soluble in NMP and DMAc.

To clarify the cause of the poor solubility of **PI-5**, wide-angle X-ray diffraction (WAXD) studies were performed because a crystalline domain can influence the solubility of the polymer [31]. The X-ray diffractograms of **PI-1** and **PI-3** showed broad diffraction curves without obvious peak features, indicating that the PIs have an amorphous morphology in principle (**Figure 10**). On the other hand, the X-ray diffraction curve of **PI-5** exhibited a relatively unambiguous peak around 17°, which indicated that **PI-5** has a more ordered phase compared to the other soluble PIs. This is likely related to the highly linear and rigid chain structure of **PI-5**, which induced high intermolecular interactions, resulting in a decrease of the solubility.

The soluble PIs of **PI-1**, **PI-2**, **PI-3**, and **PI-4** could be processed into flexible and tough films conveniently by casting from the DMAc polymer solutions. While **PI-2**, **PI-3**, and **PI-4** produced transparent films, **PI-1** generated a turbid film which appeared as the solvent was evaporated. **Table 3** shows the mechanical properties of the PI films. The PI films had tensile strength levels, elongation at break values, and a Young's modulus in the ranges of 92–145 MPa, 26–55%, and 2.1–3.2 GPa, respectively. These values were comparable to the mechanical strength of the PIs prepared from 2,2′-bis(trifluoromethyl)benzidine [22] and also indicated that the PI films are strong enough for use.

The thermal properties of the PIs were evaluated by TGA, DSC, and TMA, and these results are summarized in **Table 4**. The dynamic TGA result showed high thermal stability in which 5% weight loss occurred for the PIs in the range of

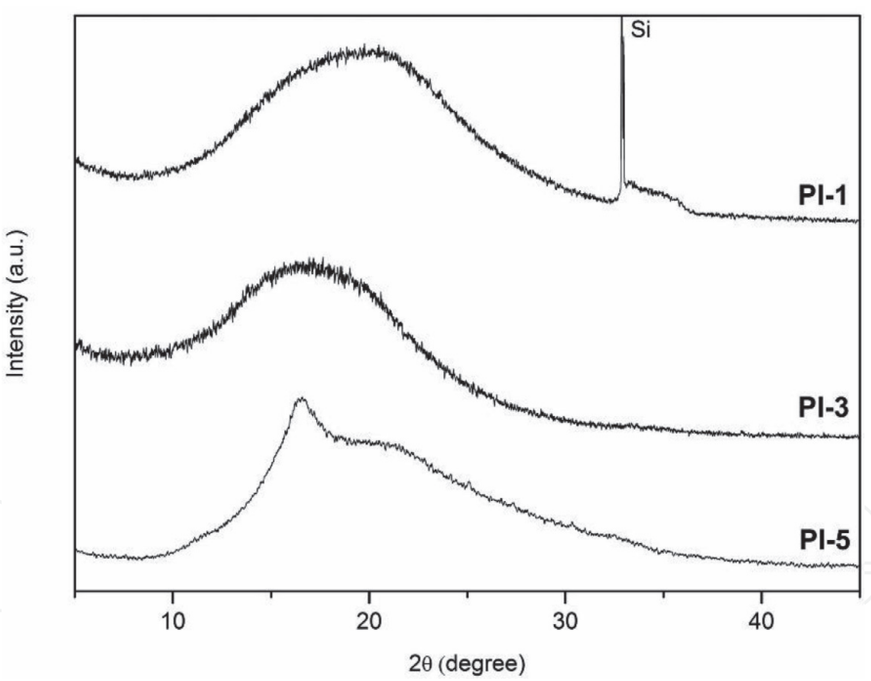

Figure 10.
*Wide-angle X-ray diffractograms of **PI-1** (film), **PI-3** (film), and **PI-5** (powder).*

Polymer code	Tensile strength (MPa)	Elongation at break (%)	Young's modulus (GPa)
PI-1	145	26	3.2
PI-2	125	55	2.8
PI-3	92	35	2.1
PI-4	95	39	2.6

Table 3.
Mechanical properties of the PI films.

Polymer code	T_{d5} (°C)[a]		T_g (°C)[b]	CTE (ppm/°C)[c]		Cutoff wavelength (nm)	Transmittance at 550 nm (%)
	In N_2	In air		2nd run	3rd run		
PI-1	604	594	366[d]	6.8	6.8	398	34
PI-2	581	553	348	42.0	42.5	371	87
PI-3	589	566	345	52.6	51.9	368	89
PI-4	535	523	362	63.1	63.0	354	90
PI-5	605	569	—[e]	—[f]	—[f]	—[f]	—[f]

[a]*5% weight loss temperature measured by TGA at a heating rate of 10°C/min.*
[b]*Measured by DSC (the second scan) in N_2 at a heating rate 10°C/min.*
[c]*A TMA analysis was conducted three times for each sample at a heating rate of 5°C/min in a heating range up to 300° C. Each CTE value was calculated from the mean coefficient of the linear thermal expansion over a specific temperature range between 50 and 250°C in the second and third runs, respectively.*
[d]*Measured by TMA at a heating rate of 5°C/min.*
[e]*Not detected.*
[f]*Not measured.*

Table 4.
Thermal and optical properties of the PIs.

535–605°C in nitrogen and 523–594°C in air (**Figure 11a** and **b**, respectively). DSC experiments were conducted at a heating rate of 10°C/min in nitrogen (**Figure 11c**). A survey of all of the PIs by DSC revealed that no endothermic peaks associated with melting were observed up to the temperature region investigated here. Moreover, while the glass-transition temperatures (T_g) of **PI-2**, **PI-3**, and **PI-4** were clearly detected, **PI-1** and **PI-5** did not show any discernible glass transition on the DSC thermograms. Therefore, the T_g of **PI-1** was measured by the TMA method after preparation of the polymer film (**Figure 11d**). All PIs exhibited high T_g values above 340°C which depended on the chemical structure of the aromatic dianhydride component. **PI-1** obtained from BPDA showed the highest T_g value (366°C) among the soluble PIs owing to the absence of a flexible linkage between the phthalimide units. Compared with PIs derived from 4-(4′-aminophenoxy)-3,5-bis(trifluoromethyl)aniline [40], the PIs based on 2,6-bis(trifluoromethyl)benzidine possess higher T_g values due to their greater chain rigidity. Even when compared to the PIs derived from 2,2′-bis(trifluoromethyl)benzidine [18–22, 25], the PIs synthesized here showed similar or higher T_g values. For example, the PIs based on BPDA and 6-FDA with 2,2′-bis(trifluoromethyl)benzidine exhibited T_g values of 287–373°C and 335°C, respectively. This result could be attributed to the unsymmetrical introduction of the two CF_3 groups, which further increases the rotational barrier of the polymer chains compared to the symmetrically introduced case.

The coefficients of thermal expansion (CTEs) of the PI films were found in the range of 6.8–63.1 ppm/°C. In general, polymers consisting of rod-like backbone structures together with a high chain alignment toward the direction parallel to the film plane have shown relatively low CTE values [24–28]. The relationship between the chain rigidity/degree of in-plane orientation and the CTE value can be applied to this study. The CTE value of the PIs decreased from 63.1 to 6.8 ppm/°C with an increase in the chain rigidity and the degree of in-plane orientation, as identified through the birefringence value (**Table 5**). Although the birefringence value of **PI-1** could not be measured due to the low transparency in this case, it can be speculated that **PI-1** has the highest degree of in-plane orientation because **PI-1** possesses the most rigid chain structure among the soluble PIs [18, 19, 24, 25, 28–30]. Therefore, **PI-1** gave the lowest CTE value (6.8 ppm/°C), displaying good dimensional stability.

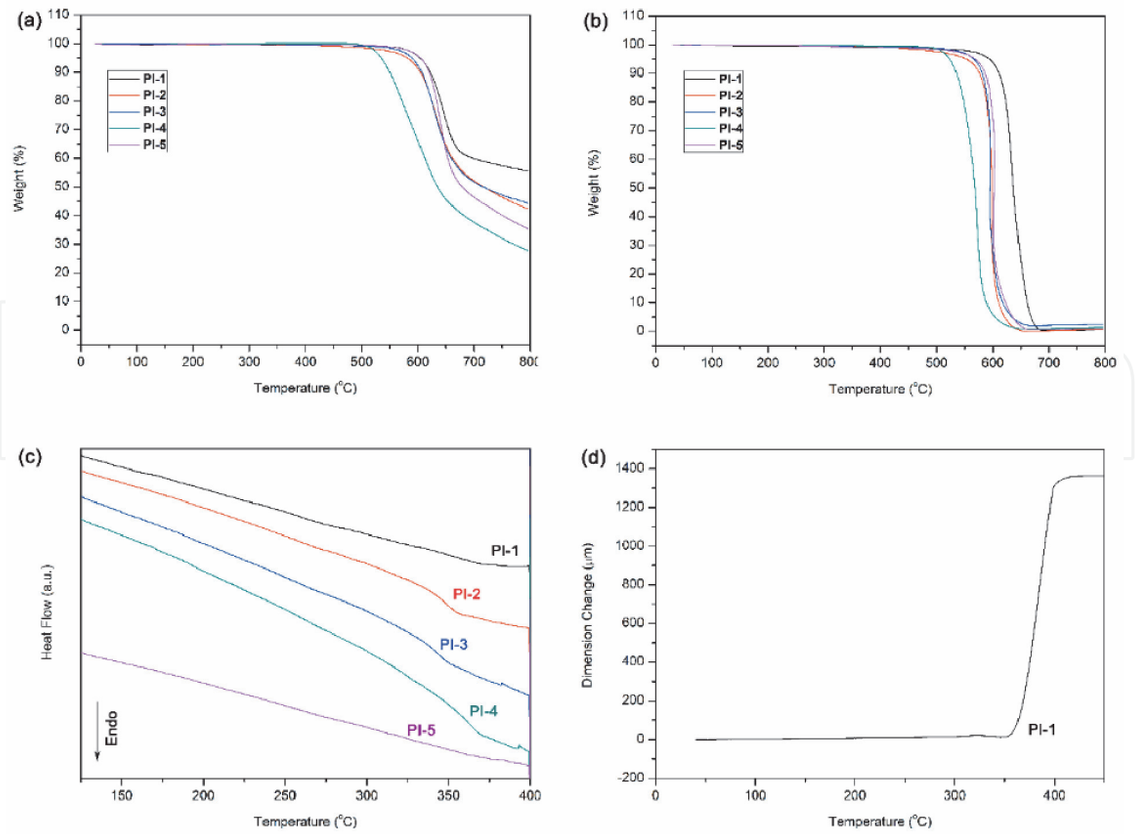

Figure 11.
TGA curves of the PIs in (a) nitrogen and (b) air at a heating rate of 10°C/min, (c) DSC curves of the PIs (the second heating run ranging from 0 to 400°C at a heating rate of 10°C/min in N_2) and (d) TMA CURVE Of ***PI-1*** *(measured at a heating rate of 5°C/min).*

Polymer code[a]	n_{TE}[b]	n_{TM}[c]	n_{av}[d]	Δn[e]	ε[f]	d (μm)[g]
PI-2	1.638	1.566	1.614	0.072	2.87	4.7
PI-3	1.619	1.561	1.600	0.058	2.82	3.1
PI-4	1.548	1.506	1.534	0.042	2.59	3.8

[a]*Measured at a wavelength of 633 nm at room temperature.*
[b]n_{TE}*: the in-plane refractive index.*
[c]n_{TM}*: the out-of plane refractive index.*
[d]n_{av}*: the average refractive index* ($n_{av} = (2n_{TE} + n_{TM})/3$).
[e]Δn*: birefringence* ($n_{TE} - n_{TM}$).
[f]*Dielectric constant estimated from the refractive index:* $\varepsilon \approx 1.10 n_{av}^2$.
[g]*Film thickness for the refractive index measured.*

Table 5.
Refractive indices of the PIs.

The corresponding UV-vis spectra of the PI films with a thickness of about 60–80 μm are shown in **Figure 12a**. While the light transparencies of **PI-2**, **PI-3**, and **PI-4** were as high as 87–90% at a wavelength of 550 nm, **PI-1** film exhibited extremely low transparency of 34%. This outcome is attributable to the high degree of in-plane orientation caused by the most rigid chain structure compared to other PIs. The cutoff wavelengths (λ_o) of the PI films listed in **Table 4** range from 354 to 398 nm, indicating that they are light-colored films. The color of the PI films decreased in the following order: **PI-1** > **PI-2** > **PI-3** > **PI-4**. As shown in **Figure 12b**, **PI-3** and **PI-4** produced fairly transparent and almost colorless PI films compared to the other PIs. The good optical properties of **PI-3** and **PI-4** were attributed to the poor CTC formation ability caused by the ether chain of ODPA and the bulky hexafluoroisopropylidene group of

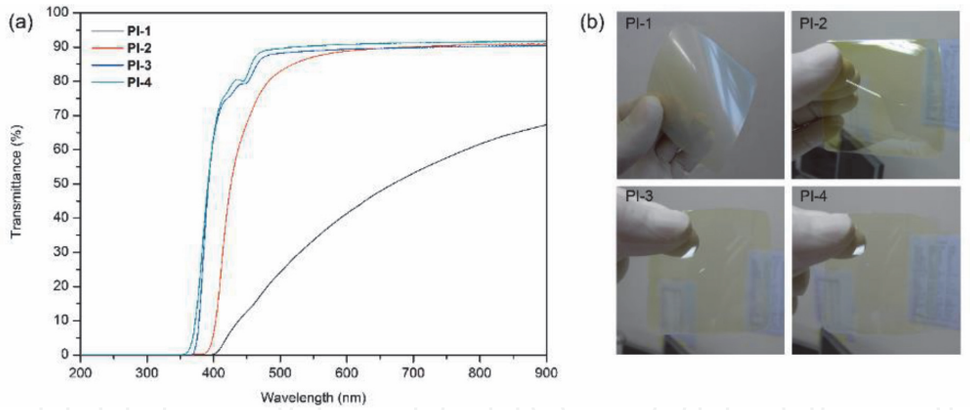

Figure 12.
(a) Transmittance UV-vis spectra and (b) photographs of the PI films.

6-FDA, respectively. The increased yellowness of **PI-2** resulted from the presence of the carbonyl group, attracting electrons in the dianhydride units.

The refractive indices and birefringence values of the **PI-2**, **PI-3**, and **PI-4** were measured using a prism-coupling method with a laser beam having a wavelength of 633 nm. The measurement of the **PI-1** film could not be performed due to the low transparency of the film. As shown in **Table 5**, the PIs showed low refractive indices (n_{av}) in the range of 1.534–1.614 due to the incorporation effect of the two CF_3 groups, which led to low molecular polarizability and density levels. The birefringence (Δn) values of the PIs were determined as the difference between n_{TE} and n_{TM} and were in the range of 0.042–0.072. The birefringence values among the PIs tested increased with an increase of the chain rigidity because the high chain rigidity led to high chain alignment in the direction parallel to the film plane [28–30]. **PI-4** showed the lowest birefringence value, indicating that the linear polarizability and segmental orientation of **PI-4** are the most isotropic among the PIs. The dielectric constant (ε) can be estimated from the refractive index n according to Maxwell's equation, $\varepsilon \approx n^2$. The ε value at 1 MHz was determined to be $\varepsilon \approx 1.10\ n_{av}{}^2$, including an additional contribution of approximately 10% due to infrared absorption [49]. The ε values of the PI films estimated from the average refractive indices ranged from 2.59 to 2.87. The low dielectric constants are also attributed to the existence of two CF_3 groups in the main chain.

In our previous work, the thermo-responsive behavior of PIs containing CF_3 groups was observed in acetyl-containing solvents [41]. Likewise, **PI-2** and **PI-3** also showed LCST behavior in the solvents used here. The transmittance of the ethyl acetate solutions of **PI-2** and **PI-3** was followed as a function of the temperature at a heating/cooling rate of 0.5°C/min. With an increase of the solution temperature, the solutions clearly turned turbid and opaque, indicating a phase transition. The clouding point temperatures (T_{cp}) of the **PI-2** and **PI-3** solutions were 44 and 48°C, respectively, at a concentration of 0.1 wt%, and the T_{cp} values decreased with an increase of the polymer concentrations. Compared to the polymers synthesized from 4-(4′-aminophenoxy)-3,5-bis(trifluoromethyl) aniline, **PI-2** and **PI-3** have lower T_{cp} values, presumably due to lower solubility originating from the increased chain rigidity. The solutions became clear and transparent again when they were cooled.

4. Conclusion

New fluorinated PIs were prepared from the benzidine monomer containing two trifluoromethyl groups on one aromatic ring, 2,6-bis(trifluoromethyl) benzidine.

Due to the rigid and twisted structure of the diamine monomer, the resulting PIs showed good solubility together with high thermal stability and excellent mechanical properties. The PIs also possessed low refractive indices and low dielectric constants due to the high fluorine contents. These PIs can be considered as promising processable high-temperature materials that can find applications in flexible electronics including substrates of flexible and rollable AMOLED displays and low-k dielectrics for microelectronics.

Acknowledgements

This work was supported by Technology Innovation Program (20007228, High transparent and heat-resistant fluorine polyimide technology for OLED substrate) funded by the Ministry of Trade, Industry & Energy (MOTIE, Korea).

Author details

Sun Dal Kim[1,2], Taejoon Byun[1], Jin Kim[2], Im Sik Chung[3] and Sang Youl Kim[1*]

1 Department of Chemistry, Korea Advanced Institute of Science and Technology (KAIST), Daejeon, Korea

2 Agency for Defense Development (ADD), Daejeon, Korea

3 Polymer and Nanomaterial Research Part, Korea Research Institute of Bioscience and Biotechnology (KRIBB), Daejeon, Korea

*Address all correspondence to: kimsy@kaist.ac.kr

References

[1] Ghosh MK, Mittal KL. Polyimides Fundamentals and Applications. New York: Marcel Decker; 1996

[2] Wilson D, Stenzenberger HD, Hergenrother PM. Polyimides. Glasgow and London: Blackie; 1990

[3] Wong WS, Salleo A. Flexible Electronics Materials and Applications. New York: Springer; 2009

[4] Liaw DJ, Wang KL, Huang YC, Lee KR, Lai JY, Ha CS. Advanced polyimide materials: Syntheses, physical properties and applications. Progress in Polymer Science. 2012;**37**:907-974

[5] Hasegawa M, Horie K. Photophysics, photochemistry, and optical properties of polyimides. Progress in Polymer Science. 2001;**26**:259-335

[6] Dhara MG, Banerjee S. Fluorinated high-performance polymers: Poly (arylene ethers) and aromatic polyimides containing trifluoromethyl groups. Progress in Polymer Science. 2010;**35**:1022-1077

[7] Ding M. Isomeric polyimides. Progress in Polymer Science. 2007;**32**: 623-668

[8] Kim SD, Lee S, Lee H, Kim SY, Chung IS. New soluble polyamides and polyimides containing polar functional groups: Pendent Pyrazole rings with amino and Cyano groups. Designed Monomers and Polymers. 2016;**19**: 227-235

[9] Hougham G, Tesoro G, Shaw J. Synthesis and properties of highly fluorinated polyimides. Macromolecules. 1994;**27**:3642-3649

[10] Hedrick JL, Carter KR, Cha HJ, Hawker CJ, Dipietro RA, Labadie JW, et al. High-temperature polyimide nanofoams for microelectronic applications. Reactive and Functional Polymers. 1996;**30**:43-53

[11] Sen SK, Banerjee S, Tg H. Processable fluorinated polyimides containing benzoisoindoledione unit and evaluation of their gas transport properties. RSC Advances. 2012;**2**: 6274-6289

[12] Chung IS, Park CE, Ree M, Kim SY. Soluble polyimides containing benzimidazole rings for interlevel dielectrics. Chemistry of Materials. 2001;**13**:2801-2806

[13] Lin SH, Li F, Cheng SZD, Harris FW. Organo-soluble polyimides: Synthesis and polymerization of 2,2-bis (trifluoromethyl)-4,4,5,5-biphenyltetracarboxylic dianhydride. Macromolecules. 1998;**31**:2080-2086

[14] Yang CP, Hsiao SH, Chen KH. Organosoluble and optically transparent fluorine-containing polyimides based on 4,4-bis amino-2-trifluoromethylphenoxy-3,3,5,5-tetramethylbiphenyl. Polymer. 2002;**43**:5995-6104

[15] Satoh A, Morikawa A. Synthesis and characterization of aromatic polyimides containing trifluoromethyl group from bis(4-amino-2-trifluoromethylphenyl) ether and aromatic tetracarboxylic dianhydrides. High Performance Polymers. 2010;**22**:412-427

[16] Cheng SZD, Wu Z, Eashoo M, Hsu SLC, Harris FWA. High-performance aromatic polyimide fibre: 1. Structure, properties and mechanical-history dependence. Polymer. 1991;**32**: 1803-1810

[17] Matsuura T, Yamada N, Nishi S, Hasuda Y. Polyimides derived from 2,2-bis (trifluoromethyl)-4,4′-diaminobiphenyl. 3. Property control for polymer blends and copolymerization of fluorinated

polyimides. Macromolecules. 1993;**26**: 419-423

[18] Matsuura T, Hasuda Y, Nishi S, Yamada N. Polyimide derived from 2,2-bis(trifluoromethyl)-4,4′-diaminobiphenyl. 1. Synthesis and characterization of polyimides prepared with 2,2-bis(3,4-dicarboxyphenyl) hexafluoropropane dianhydride or pyromellitic dianhydride. Macromolecules. 1991;**24**:5001-5005

[19] Feiring A, Auman BC, Wonchoba ER. Synthesis and properties of fluorinated polyimides from novel 2,2-bis(fluoroalkoxy)benzidines. Macromolecules. 1993;**26**:2779-2784

[20] Li F, Ge JJ, Honigfort PS, Fang S, Chen JC, Harris FW, et al. Dianhydride architectural effects on the relaxation behaviors and thermal and optical properties of Organo-soluble aromatic polyimide films. Polymer. 1999;**40**: 4987-5002

[21] Rozhanskii I, Okuyama K, Goto K. Synthesis and properties of polyimides derived from isomeric biphenyltetracarboxylic dianhydrides. Polymer. 2000;**41**:7057-7065

[22] Hergenrother PM, Watson KA, Smith JG Jr, Connell JW, Yokota R. Polyimides from 2,3,3,4-biphenyltetracarboxylic dianhydride and aromatic diamines. Polymer. 2002; **43**:5077-5093

[23] Matsuura T, Ishizawa M, Hasuda Y, Nishi S. Polyimides derived from 2,2-bis (trifluoromethyl)-4,4-diaminobiphenyl. 2. Synthesis and characterization of polyimides prepared from fluorinated benzenetetracarboxylic dianhydrides. Macromolecules. 1992;**25**:3540-3545

[24] Ishii J, Takata A, Oami Y, Yokota R, Vladimirov L, Hasegawa M. Spontaneous molecular orientation of polyimides induced by thermal imidization (6). Mechanism of negative In-plane CTE generation in non-stretched polyimide films. European Polymer Journal. 2010;**46**:681-693

[25] Arnold FE Jr, Cheng SZD, Hsu SLC, Lee CJ, Harris FW. Organo-soluble, segmented rigid-rod polyimide films: 2. Properties for microelectronic applications. Polymer. 1992;**33**: 5179-5185

[26] Eashoo M, Shen D, Wu Z, Lee CJ, Harris FW, Cheng SZD. High-performance aromatic polyimide fibres: 2 thermal mechanical and dynamic properties. Polymer. 1993;**34**:3209-3215

[27] Chuang KC, Kinder JD, Hull DL, McConville DB, Youngs WJ. Rigid-rod polyimides based on noncoplanar 4,4-biphenyldiamines: A review of polymer properties vs configuration of diamines. Macromolecules. 1997;**30**:7183-7190

[28] Terui Y, Matsuda S, Ando S. Molecular structure and thickness dependence of chain orientation in aromatic polyimide films. Journal of Polymer Science Part B: Polymer Physics. 2005;**43**:2109-2120

[29] Wakita J, Jin S, Shin TJ, Ree M, Ando S. Analysis of molecular aggregation structures of fully aromatic and Semialiphatic polyimide films with synchrotron grazing incidence wide-angle X-ray scattering. Macromolecules. 2010;**43**:1930-1941

[30] Matsuura T, Ando S, Sasaki S, Yamamoto F. Polyimides derived from 2,2-bis(trifluoromethyl)-4,4-diaminobiphenyl. 4. Optical properties of fluorinated polyimides for optoelectronic components. Macromolecules. 1994;**27**:6665-6670

[31] Kim SD, Ka D, Chung IS, Kim SY. Poly(arylene ethers) with low refractive indices: Poly(biphenylene oxide)s with trifluoromethyl pendant groups via a meta-activated nitro displacement

reaction. Macromolecules. 2012;**45**: 3023-3031

[32] Chung IS, Kim SY. Meta-activated Nucleophilic aromatic substitution reaction: Poly(biphenylene oxides) with trifluoromethyl pendent groups via nitro displacement. Journal of the American Chemical Society. 2001;**123**: 11071-11072

[33] Chung IS, Kim SY. Poly(arylene ether)s via nitro displacement reaction: Synthesis of poly(biphenylene oxides) containing trifluoromethyl groups from AB type monomers. Macromolecules. 2000;**33**:9474-9476

[34] Liu Y, Xing Y, Zhang Y, Guan S, Zhang H, Wang Y, et al. Novel soluble fluorinated poly(ether imide)s with different pendant groups: Synthesis, thermal, dielectric, and optical properties. Journal of Polymer Science Part A: Polymer Chemistry. 2010;**48**: 3281-3289

[35] Liu B, Hu W, Matsumoto T, Jiang Z, Ando S. Synthesis and characterization of organosoluble ditrifluoromethylated aromatic polyimides. Journal of Polymer Science Part A: Polymer Chemistry. 2005;**43**:3018-3029

[36] Long TM, Swager TM. Molecular design of free volume as a route to low-κ dielectric materials. Journal of the American Chemical Society. 2003;**125**: 14113-14119

[37] Lee B, Byun T, Kim SD, Kang HA, Kim SY, Chung IS. Soluble para-linked aromatic polyamides with pendent groups. Macromolecular Research. 2015; **23**:838-843

[38] Kim SD, Byun T, Lee B, Kim SY, Chung IS. Rigid-rod polyamides from 3,3-bis-(trifluoromethyl)-4,4-diamino-1,1-biphenyl. Macromolecular Chemistry and Physics. 2015;**216**: 1341-1347

[39] Chung IS, Kim KH, Lee YS, Kim SY. Poly(arylene ether)s with trifluoromethyl groups via meta-activated nitro displacement reaction. Polymer. 2010;**51**:4477-4483

[40] Kim SD, Kim SY, Chung IS. Soluble and transparent polyimides from unsymmetrical diamine containing two Trifluoromethyl groups. Journal of Polymer Science Part A: Polymer Chemistry. 2013;**51**:4413-4422

[41] Kim SD, Kim SY, Chung IS. Unprecedented lower critical solution temperature behavior of polyimides in organic media. Macromolecules. 2014; **47**:8846-8849

[42] Chern YT, Tsai JY. Low dielectric constant and high organosolubility of novel polyimide derived from unsymmetric 1,4-bis(4-aminophenoxy)-2,6-di-tert-butylbenzene. Macromolecules. 2008; **41**:9556-9564

[43] Choi H, Chung IS, Hong K, Park CE, Kim SY. Soluble polyimides from unsymmetrical diamine containing benzimidazole ring and trifluoromethyl pendent group. Polymer. 2008;**49**: 2644-2649

[44] Kim M, Kim SY. Curable aromatic polyimides containing enaminonitrile groups. Macromolecules. 2002;**35**: 4553-4555

[45] Chung IS, Kim SY. Soluble polyimides from unsymmetrical diamine with trifluoromethyl pendent group. Macromolecules. 2000;**33**: 3190-3193

[46] Hsiao SH, Guo W, Chung CL, Chen WT. Synthesis and characterization of novel fluorinated polyimides derived from 1,3-bis(4-amino-2-trifluoromethylphenoxy) naphthalene and aromatic dianhydrides. European Polymer Journal. 2010;**46**: 1878-1890

[47] Kim SD, Lee S, Heo J, Kim SY, Chung IS. Soluble polyimides with trifluoromethyl pendent groups. Polymer. 2013;**54**:5648-5654

[48] Kim SD, Lee B, Byun T, Chung IS, Park J, Shin I, et al. Poly(amide-imide) materials for transparent and flexible displays. Science Advances. 2018;**4**: eaau1956

[49] Wooten F. Optical Properties of Solids. New York: Academic Press; 1972